

# Regurgitant Flow Field Characteristics of the St. Jude Bileaflet Mechanical Heart Valve under Physiologic Pulsatile Flow Using Particle Image Velocimetry

\*Keefe B. Manning, \*Vinayak Kini, †Arnold A. Fontaine, †Steven Deutsch, and \*John M. Tarbell

*\*Department of Bioengineering; and †Applied Research Laboratory, Artificial Heart Laboratory, The Pennsylvania State University, University Park, PA, U.S.A.*

---

**Abstract:** The regurgitant flow fields of clinically used mechanical heart valves have been traditionally studied in vitro using flow visualization, ultrasound techniques, and laser Doppler velocimetry under steady and pulsatile flow. Detailed investigation of the forward and regurgitant flow fields of these valves can elucidate a valve's propensity for blood element damage, thrombus formation, or cavitation. Advances in particle image velocimetry (PIV) have allowed its use in the study of the flow fields of prosthetic valves. Unlike other flow field diagnostic systems, recent work using PIV has been able to relate particular regurgitant flow field characteristics of the Bjork-Shiley Monostrut valve to a propensity for cavitation. In this study, the

regurgitant flow field of the St. Jude Medical bileaflet mechanical heart valve was assessed using PIV under physiologic pulsatile flow conditions. Data collected at selected time points prior to and after valve closure demonstrated the typical regurgitant jet flow patterns associated with the St. Jude valve, and indicated the formation of a strong regurgitant jet, in the B-datum plane, along with twin vortices near the leaflets. Estimated ensemble-average viscous shear rates suggested little potential for hemolysis when the hinge jets collided. However, the vortex motion near the occluder tips potentially provides a low-pressure environment for cavitation. **Key Words:** Heart valve—Particle image velocimetry—Regurgitation—Cavitation.

---

Mechanical heart valves, specifically bileaflet valves, are widely used to replace diseased native valves. These prosthetic valve replacements exhibit good long-term mechanical durability but can suffer functionally from increased blood element damage, a strong propensity for thrombus formation, and a need to maintain an anticoagulant drug therapy. In vitro evaluation of near-valve flow fields can help identify characteristics that can contribute to these problems. In vitro studies have been instrumental in coupling the fluid dynamics of prosthetic valve designs to their observed clinical problems and have played a major role in the refinement of later valve designs. Ellis et al. (1) have noted that retrograde or regurgitant flow must be particularly scrutinized to

assess its impact on mechanical heart valve function. These authors investigated the flow fields in the immediate vicinity of a hinge in the St. Jude Medical (SJM) and Medtronic Parallel bileaflet valves using laser Doppler velocimetry (LDV). In the present study, we extend the work of Ellis et al. (1) and provide an evaluation of the regurgitant flow regions to assess the severity of flow structures near the valve seat as well as one diameter proximal to the valve showing the extent of the hinge jets that may potentially be linked to hemolysis and platelet activation. Flow features relevant to cavitation along the B-datum line that may contribute to hemolysis and platelet activation are also revealed (2–4).

For cavitation to occur, the local fluid pressure must drop below the vapor pressure, allowing vapor to be released through cavity growth in the form of bubbles. The drop in local pressure can result from characteristics in the local flow fields or from mechanical function of the valve. Relatively high-speed regurgitant jets or concentrated vortices can be

---

Received September 2002; revised November 2002.

Address correspondence and reprint requests to Dr. John M. Tarbell, Artificial Heart Laboratory, The Pennsylvania State University, 205 Hallowell Building, University Park, PA 16802, U.S.A. E-mail: jmt@psu.edu

associated with local pressure below the fluid vapor pressure (5). Mechanical rebound of the occluders can generate localized tension waves in the fluid, producing local low-pressure regions. Typically, after bubble growth at low pressure, the pressure recovers and the bubbles collapse back into the liquid. The collapse of cavitation bubbles has been implicated in the destruction of blood elements (2) as well as damaging occluder material (6). Particle image velocimetry (PIV) has revealed vortex formation associated with the major orifice side of the Bjork-Shiley Monostrut (BSM) mechanical heart valve, where cavitation is often observed (4). The vortices contribute to a further reduction in the local pressure during valve rebound and provide a fluid mechanical environment conducive to vortex cavitation (7).

Recent advances in PIV have enabled its use as a diagnostic tool for studying the flow field characteristics of mechanical heart valves (4,8–11). Though PIV still trails LDV in frequency response, advances in optics, CCD imaging technology, electronics (triggering), and processing techniques have improved the spatial resolution of commercial systems and their ability to capture flow field information in unsteady flows. Lim et al. used PIV to examine flow fields downstream of prosthetic and bioprosthetic heart valves, showing the viability of this approach (9,10). Browne et al. (11) evaluated the forward flow field of an SJM valve under steady flow conditions using PIV and provided a comparison of the PIV results with LDV acquired data. In their study, average velocity maps (typically 30 images) were comparable using both techniques, with, as expected, the accuracy increasing with the number of PIV images used for averaging. Kini et al. (4,8) demonstrated the effectiveness of using PIV to evaluate the regurgitant flow fields associated with mechanical heart valves, and was able to link flow field characteristics to cavitation potential. The current study uses PIV to evaluate flow structures within the regurgitant flow field of a St. Jude Medical bileaflet mechanical heart valve under physiologic pulsatile flow. The measured flow field structures will be assessed as to their potential for blood element damage or cavitation.

## METHODS

The experiments were conducted in the “single shot” experimental in vitro chamber (Fig. 1), previously described by Kini et al. (8). The single shot model simulated the reverse flow characteristics of the cardiac cycle with minimal forward flow through the valve. Thus, the net flow through the chamber was

zero. To provide optical access, the chamber was manufactured from acrylic with an optical grade glass window used as a laser window. The optical grade glass window reduced optical distortion of the light sheet and prevented damage induced by the transmission of the high-energy laser light. The smaller ventricular chamber, shown in Fig. 1, was sealed and connected to a pneumatic pressure system. The larger atrial chamber remained exposed to the atmosphere. An anodized aluminum valve holder was placed between the chambers and securely held the prosthetic mitral valve (St. Jude Medical bileaflet, 27 mm, carbon occluder with a rubber ring) under study. The rubber ring material has been used to mount an SJM valve in a prior study, with significant cavitation observed (12). The axes used in subsequent analysis are illustrated in Fig. 2. The central plane of the valve was defined as  $z = 0$ . The positive x-axis was measured from the edge of the valve holder and into the atrium. The y-axis was measured from the center of the valve. Optical access provided flow field measurements on the atrial side as close as 3 mm from the actual valve seat or valve housing.

The atrial pressure head measured at the valve centerline was kept nearly constant at a mean of 5–7 mm Hg. The systolic duration throughout the experiments was 300 ms. Left ventricular pressure was measured at the valve centerline, ~30 mm away from the valve seat, using a Millar Micro-Tip pressure catheter inserted into the sealed ventricle. The peak ventricular pressure was set to a physiologic level of 120 mm Hg, and the  $dp/dt$  at valve closure, calculated over the entire closure period following Chandran and Aluri (13), was ~1,200 mm Hg/s. The *instantaneous* value of  $dp/dt$  measured 20 ms before the impact of the occluder, following FDA guidelines, was ~2,200 mm Hg/s. Note that under these operating conditions, cavitation was not observed visually. The operating condition was deliberately kept in the sub-critical range because the presence of the cavitation bubbles might have impaired PIV measurements adjacent to the valve housing. Instead, the study focused on determining fluid flow structures that might explain, by inference, the presence, structure, and nature of cavitation fields in the critical range.

The blood analog fluid was a mixture of 60% water and 40% glycerol by volume, with a measured viscosity of 3.5 cP and a density of 1.1 g/cm<sup>3</sup> at room temperature. To measure the flow fields using PIV, the fluid was seeded with neutrally buoyant silver-coated 10  $\mu$ m diameter ( $\rho = 1.1$  g/cm<sup>3</sup>) hollow glass spheres (Potters Industries, Parsippany, NJ, U.S.A.) to accommodate the PIV measurements. In a complementary study, the valve closure and occluder

rebound events were recorded using a high-speed CCD camera (Kodak MotionCorder SR 10,000) recording at 3,000 fps. Exact occluder-to-valve seat impact was determined using an accelerometer (PCB Piezotronics, Depew, NY, U.S.A.) mounted on the valve holder at the periphery of the valve.

The PIV measurements were obtained with a commercially available dual laser pulsed PIV system (TSI Inc., St. Paul, MN, U.S.A.). Two Nd:YAG (Surelite II, Continuum Inc., Santa Clara CA, U.S.A.) lasers illuminated the particles in the flow field. Each laser generated a light beam in the infrared at a 1,064 nm wavelength. This beam was subsequently passed through a frequency doubler that produced light at 532 nm in the green region of the spectrum. The synchronized firing of the two lasers triggered with the dual-frame image acquisition was controlled using the Insight-Ultra PIV software (TSI Inc.) coupled with a synchronizer (TSI model 610032). The TSI software and hardware triggered the camera and controlled the shutter delay (50  $\mu$ s) to provide two images, corresponding to each laser pulse, that were frame straddled between two consecutive frames. Beam-combination optics combined with light sheet optics (cylindrical lens with a spherical focusing lens) were used to convert the two pulsed beams into pulsed light sheets with an average thickness of roughly 1 mm.

The PIV images were acquired using a PIVCAM (TSI Inc., model 630046) CCD camera with a resolution of 1,024  $\times$  1,018 pixels and a maximum speed of 30 frames/s. A Nikon AF Micro-Nikkor 60 mm lens was used to focus the region of interest of 30  $\times$  30 mm. The images were divided into interrogation zones approximately 1 mm  $\times$  1 mm square, and the PIV analysis was subsequently performed using the Insight software. The flow field maps presented represent an ensemble average of 30 instantaneous flow fields taken at specific phases of the flow cycle before and after valve closure. Two markers, placed on the valve holder and separated by 1.5 inches, were used to scale the images.

## RESULTS AND DISCUSSION

A study of steady-state regurgitant leakage in the SJM bileaflet valve was conducted using PIV. The valve was seated in the single shot chamber, and a steady 120 mm Hg head was maintained within the sealed ventricular side. The single shot chamber allowed the jets to vent into the atrial side of the chamber. PIV data was acquired in two planes orthogonal to one another, as shown in Fig. 2. The B-datum plane (x-z) was located between the leaflets.

The second plane, or central plane (x-y), was perpendicular to the B-datum plane and bisected the valve.

The steady-state regurgitant flow structures measured in this study by PIV were similar to those observed previously by Meyer et al. (14) using LDV. Figure 3 graphically illustrates the flow structures occurring during the steady-state regurgitant flow of the SJM bileaflet valve. The B-datum plane, where the leaflets close and seal together, was relatively free of leakage. The geometry of the bileaflet valve was such that the pressure gradient drove both occluders (leaflets) to the valve seat and contact was made along the B-datum plane and along the periphery between the leaflets and valve housing. This caused the seal to be tight near the B-datum plane region, and no significant leakage could be observed. The region between the hinges and the B-datum plane showed a weakening seal, and four separate peripheral leakage regions were consistently observed, as shown in Fig. 3. Critical zones of steady regurgitation appeared to be located near the four hinges. These small hinge-flow jets were directed away from each other toward the opposite hinge pair and into the atrium. Such hinge jets have been detected previously *in vivo* using color Doppler (15).

The pulsatile flow PIV images were acquired at 5 ms prior to valve impact and 5, 50, and 100 ms after impact. Figures 4–7 are the experimentally determined PIV flow patterns in the central plane during and after valve closure. Each figure consists of an average of 30 cycles at the specific time point during the valve closure event. The PIV vector maps obtained at 5 ms prior to leaflet impact (Fig. 4) exhibit a regurgitant or closure volume flow directed into the atrium characterized by a jet moving nearly 1 m/s along the center of the leaflets. The propagation and expansion of this jet into the relatively stagnant atrial fluid coupled with the motion of the leaflets produces two small tip vortices bordering on either side of the jet. Five ms after valve impact (Fig. 5), the magnitude of the peak jet velocity decreased from 1 m/s to 0.55 m/s but appeared to be more structured while the vortex motion remained. These maximum velocities correlated well with the velocities observed by Ellis et al. (1). This closure volume jet and the associated vortices dissipated 20 ms after leaflet impact. At 50 ms after impact, two strong, diverging, regurgitant flow jets appeared in the central plane, as shown in Fig. 6. These jets do not appear to develop during leaflet closure, as the left ventricular pressure rises, and are not associated with the single, closure volume jet described in Fig. 5. The jet structures illustrated in Fig. 6 contain

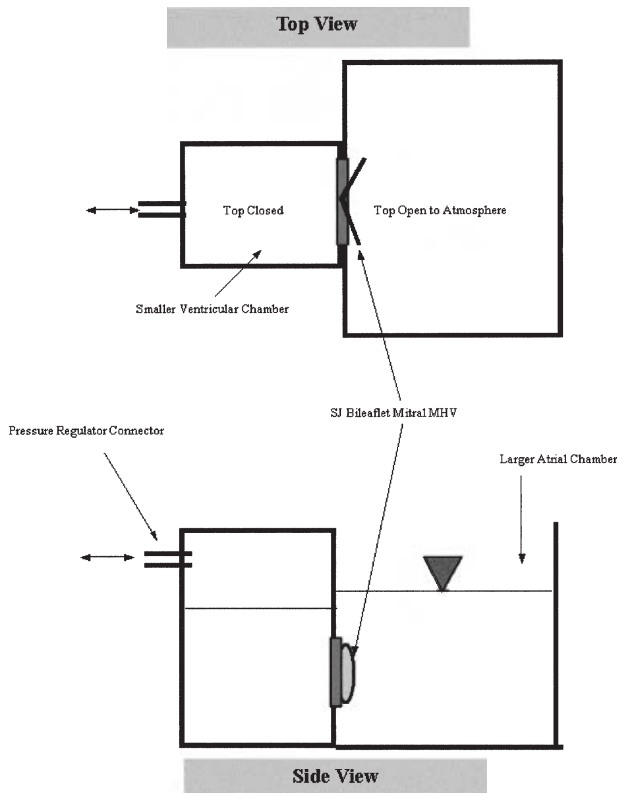


**FIG. 1.** Schematic view of the MHV chamber used for PIV studies. The diagram shows a SJM bileaflet mitral valve in the valve holder. The larger atrial chamber is held open to the atmosphere. The smaller ventricular chamber is closed and connected to a pneumatic pressure regulator. The regulator provides the systolic ejection pressure that shuts the mitral valve. The valve is then allowed to open until the fluid levels equalize. There is no true forward flow.

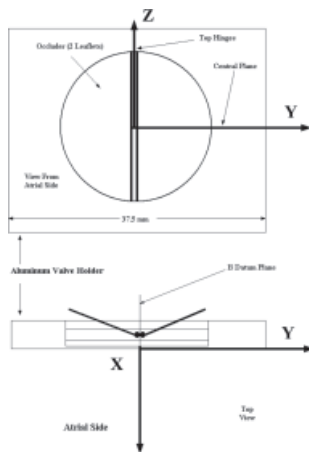


**FIG. 2.** Axes definition. The diagram shows an SJM bileaflet valve in the valve holder. The central plane of the valve was defined as  $z = 0$ . The x-axis was measured from the edge of the valve holder and into the atrium. Due to the valve holder recess and proximity of the wall, our first point is  $\sim 5$  mm from the valve seat on the atrial side. The y-axis was measured from the edge of the valve holder on one leaflet side and in the direction of the other leaflet side.

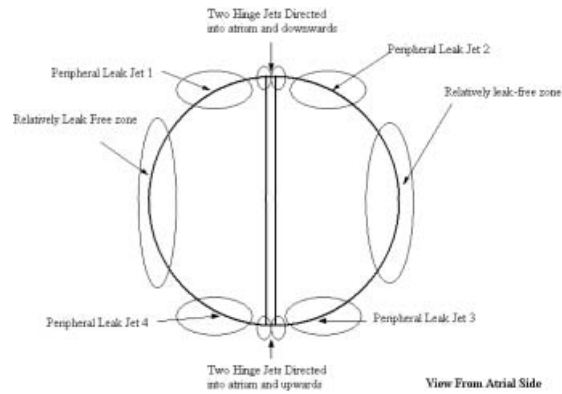


**FIG. 3.** Critical zones for the steady-leak phase along the periphery of the SJM bileaflet valve. The central plane periphery is tightly sealed and does not provide evidence of any peripheral leak jet. Two strong jets emerge from both hinges and toward one another as they enter the atrium. The regions of transition between the tightly sealed central plane and the hinge region show steady leak jets that are approximately in the valve plane.

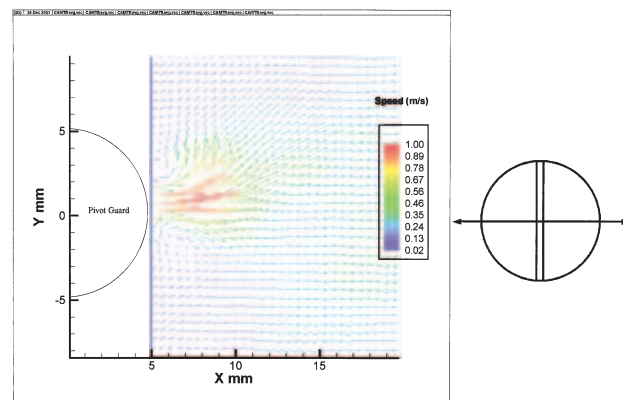


**FIG. 4.** Phase-averaged ( $n = 30$  cycles) flow patterns in the regurgitant flow past the SJM bileaflet valve in the central plane ( $z = 0$  mm) during valve closure  $\sim 5$  ms before impact. Note that the map begins  $\sim 5$  mm away from the actual valve seat.

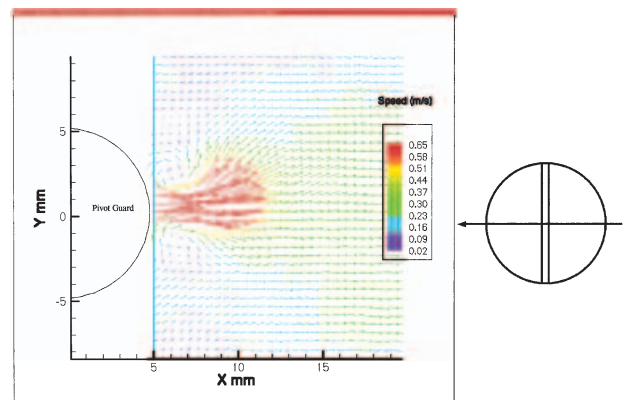


**FIG. 5.** Phase-averaged ( $n = 30$  cycles) flow patterns in the regurgitant flow past the SJM bileaflet valve in the central plane ( $z = 0$  mm)  $\sim 5$  ms after impact. Note that the map begins  $\sim 5$  mm away from the actual valve seat.

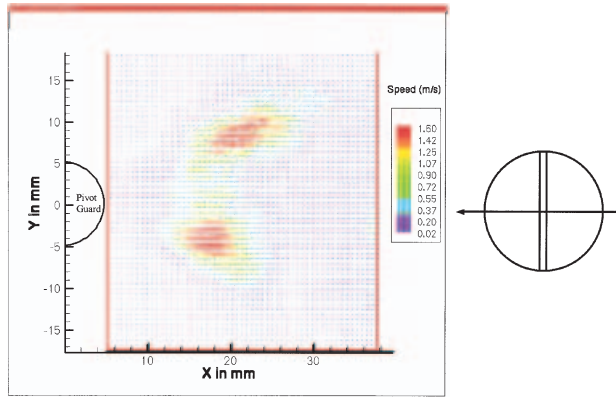


**FIG. 6.** Phase-averaged ( $n = 30$  cycles) flow patterns in the regurgitant flow past the SJM bileaflet valve in the central plane ( $z = 0$  mm)  $\sim 50$  ms after impact. Note that the map begins  $\sim 5$  mm away from the actual valve seat.

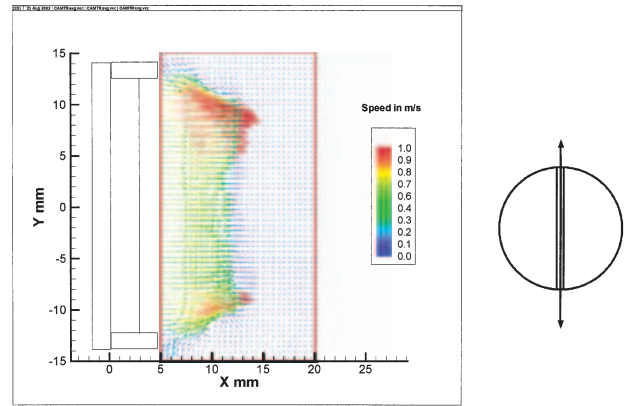


**FIG. 9.** Phase-averaged ( $n = 30$  cycles) flow patterns in the regurgitant flow past the SJM bileaflet valve in the B-datum plane ( $y = 0$  mm) during closure motion  $\sim 5$  ms after impact. Note that the map begins  $\sim 5$  mm away from the actual valve seat.

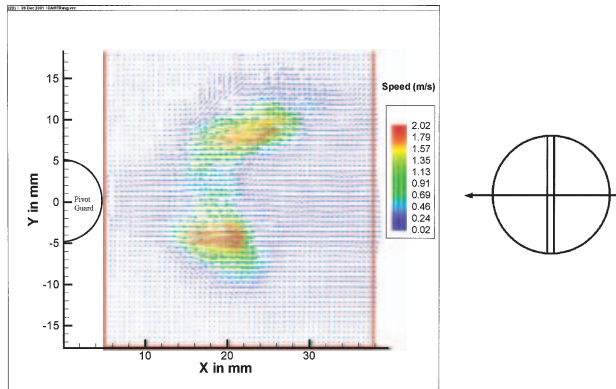


**FIG. 7.** Phase-averaged ( $n = 30$  cycles) flow patterns in the regurgitant flow past the SJM bileaflet valve in the central plane ( $z = 0$  mm)  $\sim 100$  ms after impact. Note that the map begins  $\sim 5$  mm away from the actual valve seat.

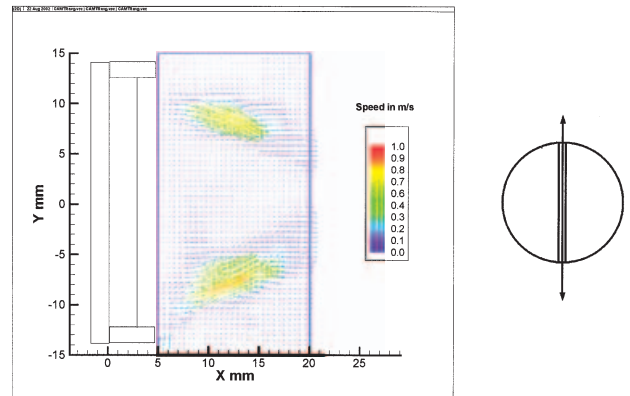


**FIG. 10.** Phase-averaged ( $n = 30$  cycles) flow patterns in the regurgitant flow past the SJM bileaflet valve in the B-datum plane ( $y = 0$  mm) during closure motion  $\sim 50$  ms after impact. Note that the map begins  $\sim 5$  mm away from the actual valve seat.

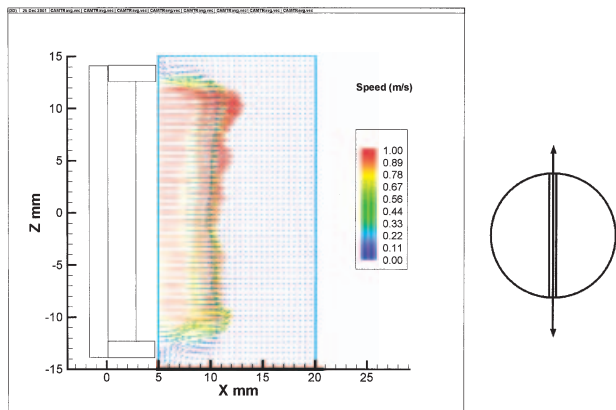


**FIG. 8.** Phase-averaged ( $n = 30$  cycles) flow patterns in the regurgitant flow past the SJM bileaflet valve in the B-datum plane ( $y = 0$  mm) during closure motion  $\sim 5$  ms before impact. Note that the map begins  $\sim 5$  mm away from the actual valve seat.

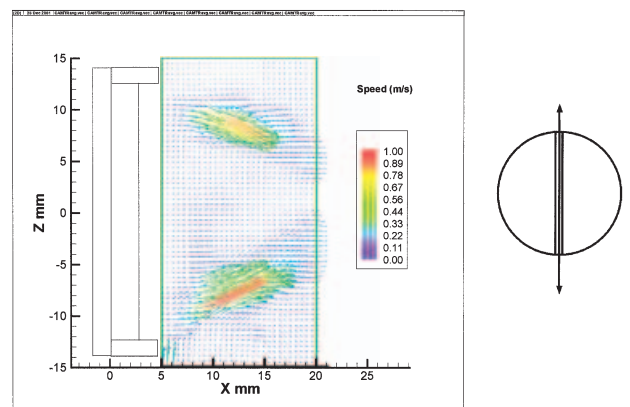


**FIG. 11.** Phase averaged ( $n = 30$  cycles) flow patterns in the regurgitant flow past the SJM bileaflet valve in the B-datum plane ( $y = 0$  mm) during closure motion  $\sim 100$  ms after impact. Note that the map begins  $\sim 5$  mm away from the actual valve seat.

only two components of the three-dimensional jets formed at the hinges. Figure 7 shows the diverging hinge jets 100 ms after impact. The maximum velocities have increased from 1.60 m/s to 2.02 m/s between 50 and 100 ms, and correspond to the increase in left ventricular pressure during this time frame. Estimated maximum viscous shear rates (stresses) around the converged hinge jets were on the order of  $500 \text{ s}^{-1}$  ( $20 \text{ dyne/cm}^2$ ), suggesting that hemolysis would not be induced by these jets in the central plane. However, the turbulent stresses are undoubtedly higher. The regurgitant jets appear to merge more than one diameter from the valve housing and are more prominently seen in the B-datum plane vector maps.

Figures 8–11 show the evolution of the closure volume and the regurgitant leakage flow, observed in the B-datum plane, emanating between the leaflets during closure and at the hinges. These PIV images were again taken 5 ms prior to valve impact and 5, 50, and 100 ms after impact. Figure 8 shows the intense nature of the hinge jets moving toward the central plane from either side of the valve 5 ms prior to valve impact along with the closure volume flow being forced between the leaflets. Five milliseconds after valve impact (Fig. 9), the closure volume flow between the leaflets is observed to decrease as the valve leaflets seat in the housing, while the regurgitant flow from the hinges remains quite strong, with jets on the order of 1 m/s. The jets emanating from the hinges moved outward away from the B-datum plane and toward the central plane. The hinge jets on opposite sides eventually merged into the central plane, as shown in Figs. 6 and 7. Figures 10 and 11, 50 and 100 ms after impact, illustrate the persistent nature of the hinge jets as they converged into the central plane one valve diameter upstream and moved through the plane. At 50 ms after valve impact (Fig. 10), the leaflets seal and the closure volume flow between the leaflets ceases. This concurs with Fig. 6, which showed little if any leakage flow between the valve leaflets. Also at 50 and 100 ms after valve impact, minor recirculation zones appeared on the outer edges of the hinge jets.

These mitral regurgitant flow patterns have been observed qualitatively using streakline photography in the Penn State left ventricular assist device (16). LDV data also revealed similar regurgitant jets in the hinge region of the SJM valve (17). The behavior of the regurgitant flow on the atrial side showed the expected pressure-driven jet and the twin vortices, similar to the jet and vortices on the major and minor orifice sides of the BSM valve (4,8). The vortices shown in Figs. 4 and 5 may provide a

low-pressure environment for the development of cavitation that has been observed along the B-datum line at closure, as demonstrated by Shu et al. (18). The vortices may be similar to the fluid mechanical environment near the edge of the BSM valve at closure where vortices are formed that provide an environment conducive to cavitation. We have previously shown that the estimated pressure drop near the center of the vortices can plunge well below the fluid vapor pressure, resulting in cavitation (7). Although the flow vector maps in these figures begin  $\sim 5 \text{ mm}$  from the valve seat, due to laser glare off the SJM housing, there was clearly an indication of strong fluid motion at 5 mm. Cavitation has also been observed around the periphery of the SJM valve (12,19). However, the flow fields adjacent to the leaflets and within 5 mm of the housing were not accessible by PIV in this study due to glare from the SJM housing. LDV would be able to image closer ( $\sim 3 \text{ mm}$ ), but mapping the entire flow field region would be tedious.

## CONCLUSIONS

Particle image velocimetry was used to investigate the regurgitant flow fields associated with the St. Jude Medical bileaflet mechanical heart valve. The images revealed sustained regurgitant flow around the hinge regions of the leaflets along with peripheral leak jets near the hinges. The hinge jets moved into the atrium, with the pairs of jets on one side joining the jets on the opposite side. Along the B-datum plane, a strong regurgitant, closure volume jet was formed, with vortices flanking either side, and persisted for  $\sim 20 \text{ ms}$  after occluder impact. The jets and twin vortices were reminiscent of regurgitant flow associated with the major and minor orifices of the BSM mechanical heart valve at closure as previously published (8). The central plane of the SJM valve showed virtually no leakage after seating of the occluders. The sustained regurgitant flow through the hinges produced two diverging jets in the central plane one diameter upstream of the valve. The PIV results correlate well with previously described streakline photography and LDV data, further demonstrating the viability of PIV as a tool to investigate mechanical heart valves.

Average viscous shear rates (stresses) around the regurgitant jets were no higher than  $500 \text{ s}^{-1}$  ( $20 \text{ dyne/cm}^2$ ), suggesting that they would not induce hemolysis. Turbulence levels were not measured, but other studies have detected Reynolds stresses up to  $1,800 \text{ dynes/cm}^2$  in regurgitant jets of the SJM valve that may contribute to hemolysis (17). Vortex

formation along the B-datum line during the 20 ms period surrounding valve closure may provide a low-pressure environment that could contribute to the formation of cavitation that has been observed at this location in other studies.

**Acknowledgments:** This research was supported through the NIH on grant HL 48652.

## REFERENCES

1. Ellis JT, Healy TM, Fontaine AA, et al. An in vitro investigation of the retrograde flow fields of two bileaflet mechanical heart valves. *J Heart Valve Dis* 1996;5:600–6.
2. Garrison LA, Lamson TC, Deutsch S, Geselowitz DB, Gaumond RP, Tarbell JM. An in vitro investigation of prosthetic heart valve cavitation in blood. *J Heart Valve Dis* 1994;3:7–24.
3. Zapanta CM, Stinebring DR, Sneckenberger DS, et al. In vivo observation of cavitation on prosthetic heart valves. *ASAIO J* 1996;42:M550–5.
4. Kini V, Bachmann C, Fontaine A, Deutsch S, Tarbell JM. Flow visualization in mechanical heart valves: occluder rebound and cavitation potential. *Ann Biomed Eng* 2000; 28:431–41.
5. Young FR. *Cavitation*. London: McGraw-Hill, 1989.
6. Kafesian R, Howanec M, Ward GD, Diep L, Wagstaff LS, Rhee R. Cavitation damage of pyrolytic carbon in mechanical heart valves. *J Heart Valve Dis* 1994;3:52–7.
7. Bachmann C, Kini V, Deutsch S, Fontaine AA, Tarbell JM. Mechanisms of cavitation and the formation of stable bubbles on the Bjork-Shiley Monostrut prosthetic heart valve. *J Heart Valve Dis* 2002;11:105–13.
8. Kini V, Bachmann C, Fontaine A, Deutsch S, Tarbell JM. Integrating particle image velocimetry and laser Doppler velocimetry measurements of the regurgitant flow field past mechanical heart valves. *Artif Organs* 2001;25:136–45.
9. Lim WL, Chew YT, Chew TC, Low HT. Steady flow dynamics of prosthetic aortic heart valves: a comparative evaluation with PIV techniques. *J Biomech* 1998;31:411–21.
10. Lim WL, Chew YT, Chew TC, Low HT. Pulsatile flow studies of a porcine bioprosthetic aortic valve in vitro: PIV measurements and shear-induced blood damage. *J Biomech* 2001;34: 1417–27.
11. Browne P, Ramuzat A, Saxena R, Yoganathan AP. Experimental investigation of the steady flow downstream of the St. Jude bileaflet heart valve: a comparison between laser Doppler velocimetry and particle image velocimetry techniques. *Ann Biomed Eng* 2000;28:39–47.
12. Bachmann CG. A brief overview of mechanical cardiac valve prostheses and an experimental investigation into the fluid mechanics at the instant of valve closure. Master's thesis, Pennsylvania State University, 2000.
13. Chandran KB, Aluri, S. Mechanical valve closing dynamics: relationship between velocity of closing, pressure transients, and cavitation initiation. *Ann Biomed Eng* 1997;25:926–38.
14. Meyer RS, Deutsch S, Maymir JC, Geselowitz DB, Tarbell JM. Three-component laser Doppler velocimetry measurements in the regurgitant flow region of a Bjork-Shiley Monostrut mitral valve. *Ann Biomed Eng* 1997;25:1081–91.
15. Yoganathan AP, Heinrich RS, Fontaine AA. Fluid dynamics of prosthetic valves. In: Otto CM, ed., *The practice of clinical echocardiology*. Philadelphia: WB Saunders Co., 1997:773–96.
16. Meyer RS. Three-component laser Doppler velocimetry measurements in the vicinity of mechanical heart valves in a mock-circulatory loop. PhD thesis, Pennsylvania State University, 1997.
17. Meyer RS, Deustch S, Bachmann CB, Tarbell JM. Laser Doppler velocimetry and flow visualization studies in the regurgitant leakage flow region of three mechanical heart valves. *Artif Organs* 2001;25:292–9.
18. Shu MCS, Leuer LH, Armitage TL, Schneider TE, Christiansen DR. In vitro observations of mechanical heart valve cavitation. *J Heart Valve Dis* 1994;3(suppl I):S85–93.
19. Graf T, Reul H, Detlefs C, Wilmes R, Rau G. Causes and formation of cavitation in mechanical heart valves. *J Heart Valve Dis* 1994;3(suppl I):S49–64.